ISSN: 2577 - 8005

Research Article

Medical & Clinical Research

# Loss of Information Associated with the Perceptomotor Cognitive Domain: Praxis

**Jair Rodrigues Neyra[1], Rafael Santos da Costa[2] and Thiago RS Moura[3]***

[1]*Faculty of Engineering, Federal University of Pará, Salinópolis Campus, Salinópolis, PA, Brazil*

[2]*Faculty of Mathematics, Federal University of Pará, Salinópolis Campus, Salinópolis, PA, Brazil*

[3]*Faculty of Physics, Federal University of Pará, Salinópolis Campus, Salinópolis, PA, Brazil*

***Corresponding author**
Thiago R.S. Moura, Faculty of Physics, Federal University of Pará, Salinópolis Campus, Salinópolis, PA, Brazil. E-mail: trsmoura@yahoo.com.br

**Submitted**: 25 Nov 2019; **Accepted**: 16 Dec 2019; **Published**: 07 Jan 2020

## Abstract

*We have proposed a random walk model to model perceptomotor cognitive domain damage in patients with neurocognitive disorders (NDs). The random walk model with truncated Lorentz memory profile. We have reported that memory damage has an impact on random walkers' praxis and, consequently, on the global diffusive process, fractal dimension and information loss, and it is the major impact on information loss. We have found two diffusive regimes: the ordinary and the superdiffusive. We have observed two superdiffusion regions separated by a region with ordinary diffusion regime: one in the anti-persistence region and one in the persistence region. These regions are characterized by diffusion level curves, invariant curves of scale variations in the Lorentz distribution. In the anti-persistence region, we found a greater variation in entropy, for example, greater loss of praxis-related information than in the persistence region. Therefore, when memory impairment is accompanied by observation of anti-persistent behavior, there are greater losses of information related to the perceptomotor domain of random walkers.*

**Keywords:** Memory, Damage, Neurocognitive Disorders, Praxis, Random Walk

## Introduction

The neurocognitive disorders (NDs) are associated with the primary clinical condition of reduced cognitive ability of the individual. NDs (neurocognitive disorders) are delirium, accompanied by major ND syndrome, minor neurocognitive disorder and different etiological subtypes. The NDs may be associated with various etiologies such as Alzheimer's disease, vascular disease, Lewy body disease, Parkinson's disease, frontotemporal disease, Huntinton's disease, prion disease, yet may be drug-induced foreign substance-induced due to traumatic brain injury caused by HIV infection, may be a consequence of multiple etiologies and may be caused by another medical condition or related to some other unspecified factor. Neurocognitive disorder is not present in the early years of life, such as invasive neurodevelopmental disorders. NDs generally affect several cognitive domains. The cognitive domains are: a) complex attention, b) learning and memory and c) perceptomotor. The domain of complex attention is related to sustained attention, split attention, selective attention, and processing speed. The learning and memory domain includes immediate memory (recent memory, track recall and recognition memory) and very long term memory. The third domain, the perceptomotor domain, is related to the ability of visual perception, visuo-constructive, perceptomotor, praxis and gnosia [1-12].

The symptoms related to neurocognitive diseases are observed by professionals (clinicians) in standard consultations, which are recorded for patient history. Each consultation, as well as the symptoms and evolution of the disease, are systematically recorded in periodic consultations over time. Therefore, symptoms are observed in an orderly manner over time. This set of observations is a collection of ordered objects over time. A collection of observations made sequentially over time is a time series. One way to model time series is from random walk representation [13-18].

Inspired by the development of new tools for analyzing, modeling and classifying neurocognitive disorders, we nonetheless report the use of random walk technique for modeling and numerical simulation of memory loss over time. The memory loss can have several etiologies. One of its origins may be dementia due to the presence of Lewy bodies. For example, Parkinson's disease shows the presence of Lewy bodies. Lewy bodies are abnormal clumps of alpha-synuclein protein [19,20]. Another pathology associated with dementia is Alzheimer's disease, which is a chronic neurodegenerative disease. Its symptoms appear in a hierarchical way, affecting regions ordinally over time. Initially, the first most common symptom that arises is recent memory loss, the picture evolves with the observation of language difficulties, reduction in recognition ability, difficulty in remembering recent events, which is in the domain of learning and memory. The progression of the disease leads the individual to loss of control of bodily functions, which is in the perceptomotor domain. Finally leading to death [21-23].

Observing the set of cognitive domains and their respective symptoms, especially the perceptomotor domain. We have modeled the perceptomotor domain pathologies from time series. To model

the time series we have used the discrete random walking class with memory [15-18]. We have simulated the memory reduction from the time-dependent truncated Lorentz distribution [24]. The narrowing of the distribution is related to reduced ability to remember past facts and decisions. Initially, the experiment is performed with the truncated Lorentz distribution capable of retrieving a certain amount of walker actions, let us say, letter ($N$). The distribution is narrowed to reduce the number of actions the walker can recover, let us say:($M < N$), which induces damage to the walker's memory. This reduction in the number of actions that the random walker can retrieve therefore impacts the walker's microscopic actions, according to the memory profile shaped by the truncated Lorenz probability distribution. The narrowing of the probability distribution is associated with short, medium and long term memory impairment in an individual with NDs (neurocognitive disorders). The changes in the microscopic behavior of random walkers, by analogy, are associated with the impact of damage on the perceptomotor domain. Therefore, to measure the impact of memory damage on the perceptomotor domain, we have measured the Hurst exponent that, for random walks, it measures the diffusion regimes. Major changes in diffusion regimes in random walks, are measured by ($H$) may be associated with greater probability distribution deformations, for example, lower ability to recover past actions. Therefore, from the perspective of NDs (neurocognitive disorders), greater memory damage may be associated with the observation of pathologies in the perceptomotor domain, for example, in the microscopic dynamics of random walkers.

The diffusion regimes can be classified by the Hurst exponent as anomalous diffusion.($H\neq 1/2$) and ordinary ($H=1/2$). We have highlighted two anomalous diffusion regimes, the subdifusive regime ($H<1/2$) and the superdifusive regime($H>1/2$). Typical measures of ($H$), at other intervals, they classify other diffusion regimes [15-18]. Each observation of the time series, let us say at the instant of time, is represented by a step of a random walker who recovers his decisions according to Lorentz's memory profile. The microscopic dynamics of the set of random walkers, in the way information is retrieved, it follows Lorentz's memory profile, which has an impact on the measurements of physical observable items.

We have chosen to build our model from memory class random walk models. The salient feature for choosing this class of random walks is retrieving memories of the past according to a certain probability distribution, which we have chosen the truncated Lorentz distribution.

## Materials and Methods

Inspired by the memory class random walk model, we have proposed a memory profile random walk model, according to the truncated Lorentz distribution [15-18,24]. In the random walk model with uniform memory profile, each step performed at the instant of time depends on the walker's entire history. Each state is retrieved equally. This is the way to shape random walks with uniform memory profile. The probability of retrieving a past decision at the instant of time $t$+1 is $1/t$.

The random tours have well-defined stochastic rules. It occurs as follows: the walker walks one step to the right +1 or one step left -1, with the stochastic evolution equation given by:

$$X_{t+1}=X_t+\sigma_{t+1} \quad (1)$$

for the instant of time $t$+1. When we decide to take a step to the right, for example, a variable $\sigma_{t+1}$ assumes the value +1 by taking a step to the left assumes the value -1. The memory formed of a set of random variables $\sigma_{t'}$ for the instant of time $t' < t$. The microscopic dynamics occur as follows:

(a) in the instant of time $t$+1, an instant of time: $t'$ is randomly chosen with uniform probability of the set: 1,2,3,...,$t$.

(b) $\sigma_{t+1}$ is determined stochastically by, $\sigma_{t+1}=\sigma_{t'}$ with probability $p$ and $\sigma_{t+1}=-\sigma_{t'}$ with probability1-$p$.

The initial moment of the walk, $t$=1, instant, where the walker performs the first step requires a single rule. In the instant of time: $t$=1, the walker is in position $X_0$, moves to the right with probability or left with probability 1-$q$, assuming the value, $\sigma_1$=+1 with probability $q$ or $\sigma_1$=-1 with probability 1-$q$. In the instant of time: $t$, the walker position is quantified by the equation:

$$X_t=X_0+\sum_{t'=1}^{t}\sigma_{t'} \quad (2)$$

The parameterpquantifies the likelihood of the walker repeating a past action at the instant of time: $t'$. For ($p>1/2$) the behavior of the walker is said to be persistent, characterized by the repetition of the same past actions. For ($p<1/2$), the walker makes a decision contrary to the decision to past decisions, this behavior is called anti-persistent. For the value of ($p=1/2$) the movement is Brownian. The first and second moments of the position are respectively:

$$\langle x(t)\rangle = \frac{\delta}{\Gamma(\lambda+1)}t^{2p-1} \quad (3)$$

$$\langle x^2(t)\rangle = \begin{cases} \frac{t}{3-4p} & ,p<\frac{3}{4} \\ tlnt & ,p=\frac{3}{4} \\ \frac{t^{4p-2}}{(3-4p)\Gamma(4p-2)} & ,p>\frac{3}{4} \end{cases} \quad (4)$$

In equation (3) we have the situation: $\delta$=2$q$-1, $\lambda$=2$p$-1 and $\Gamma$ is the gamma function. The parameters ($\delta$) e ($\lambda$) are set in the range [-1,1]. In the equation (4), note that; for($p < 3/4$) the second moment is a linear function of t, the diffusion is ordinary; for ($p > 3/4$) the second moment is a logarithmic function of t, this is the transition point between diffusive regimes; on the point ($p > 3/4$) the second time is described by a polynomial function of the system is superdifusive [15].

Our model consists of random walks with an associated memory capable of retrieving events from the past according to the memory profile described by the truncated Lorentz probability distribution function. The probability distribution is used to bring from memory at the instant: $t$+1, a reminder of the set's past: 1,2,3,...,$t$. In our model we have exchanged the uniform distribution for the truncated Lorentz distribution. This change is relevant for modeling the memory damage introduced by variations in the scale parameter of the distribution. We will explain this mechanism later. The truncated Lorentz distribution function is described by the equation below:

$$P(t') = \frac{P_0}{(\beta)^2+(t\prime-\alpha)^2}$$

in which ($\alpha = t/2$) the location parameter relative to the current time ($t$), ($\beta$) the scale parameter and $P_0$ is the normalization constant. The

Lorentz distribution is defined for our problem in the range [0,+∞). The width of the distribution is controlled by the scale parameter ($\beta$). The bigger it is ($\beta$) the greater is the number of possible actions the walker can remember; the smaller it is ($\beta$), the smaller is the number of possible actions the walker can remember, simulating memory damage.

We have measured three physical observable items: the Hurst exponent, the fractal dimension, and the entropy of information adapted to the context of random walks [25]. We have performed Hurst exponent measurements to classify diffusion regimes. The fractal dimension quantifies the roughness of the curves that emerge from random walks. The information entropy measurements are used to quantify information loss due to memory damage.

To classify the diffusive regimes in random walks, we have used the Hurst exponent. The asymptotic scale law of the mean square deviation of position in relation to time allows us to classify diffusive removals of random walkers. The mean square deviation is defined as follows: $\langle(x-\langle x\rangle)^2\rangle = t^{2H}$, in which ($H$) is the exponent of Hurst. Computational experiments necessarily imply a finite system approach. Finite systems may exhibit behaviors, observed in the measurements of the physical observables, that disappear at the asymptotic limit, which are known by the name of finite size effects. These effects are generously addressed in Statistical Mechanics research. [26-33]. In our numerical experiments of finite size random walks, the first moment of position grows slower than the second moment, implying the approximation $\langle(x-\langle x\rangle)^2\rangle \approx \langle x^2\rangle$. Therefore, the measures of ($H$) can be obtained from the relationship $\langle x^2\rangle = t^{2H}$.

The information entropy measures the overall effect of bit variation associated with random walks. The information entropy is described by the equation:

$$S = -\sum_j F_j(x,t) log_2\left(F_j(x,t)\right) \qquad (6)$$

in which $Fj\ (x,t)$ is the probability distribution of finding random walkers in the position $x$, in the instant of time: $t$, for a given scale parameter value ($\beta$).

## Results

Typical measures of ($H$) show that our results show anomalous diffusion in the persistence and anti-persistence regions. For ($p > 1/2$) the walker exhibits persistent behavior, to ($p = 1/2$) the behavior is Markovian and for ($p < 1/2$) the behavior is anti-persistent. The anomalous diffusion can be classified as superdiffusive ($H > 1/2$), normal diffusive ($H = 1/2$) and subdifusive ($H < 1/2$).

In the figure 1, typical Hurst exponent measurements are displayed as a function of the scale parameter ($\beta$) and the feedback parameter ($p$). In the figure 1, the color map of the Hurst exponent with various shades of purple is shown. The darker shades of purple are related to measurements of the Hurst exponent when ($H \to 1/2$), as lighter shades are related to values of ($H \to 1$). We have noted the emergence of the ordinary diffusive regime and the superdiffusive regime. The curves are displayed to highlight contours for which the quantitative values of the Hurst exponent remain invariant by the scale ($\beta$) and by feedback ($p$). The color map is divided into two regions by a central region, adjacent to $p \to 1/2$, is characterized by the diffusive behavior that tends to Brownian behavior, for example when ($H \to 1/2$). We observed closed and open curves with ($H = 1/2$). This region divides two other regions where we have observed the superdiffusive regime. The superdiffusive regime arises as it moves away from the center of the figure in ($p = 1/2$) for anti-persistence regions ($p < 1/2$) and persistence ($p > 1/2$). In the anti-persistence region, the superdiffusive regime arises when the memory scale varies around typical values ($\beta < 4x10^4$). Besides, we have found contours with the superdiffusion regime characterized by several intensities of superdiffusion, quantified by measures of $H$=0.6,0.7 e 0.9. Therefore, we have highlighted two regions that present a change from the ordinary diffusion regime to the superdiffusion regime. To note this transient, however, we look at the central part of the color map, the region characterized by contours with ($H \to 1/2$), moving away from it towards the anti-persistence region with scaling parameter reduction, ($\beta \to 0$) and ($p \to 0$), we have found the superdiffusion regime. Mainly, this super-diffusive regime was found in the regions where ($0 \leq p < 1/2$) and in the interval of ($0 < \beta < 4x10^4$ ). To prove the second transition of the diffusion regime, once again, starting from the central region of the map, in the vicinity of ($p = 1/2$), in the increasing sense of, from the center of the map to the persistence region ($p > 1/2$), we have found Hurst exponent curves with value spectrum ($H > 1/2$) which classifies this region as superdiffusive. We have noted that this region has equi-diffusive curves that extend throughout the system, regardless of the order of the scale parameter ($\beta$). Seeing that these curves present Hurst's exponent ($H > 1/2$), which classifies this region as superdiffusive, there is therefore a transient region of the ordinary diffusive regime ($H = 1/2$) for the superdiffusive regime ($H > 1/2$), insofar as ($p \to 1$) for all values of ($\beta$).

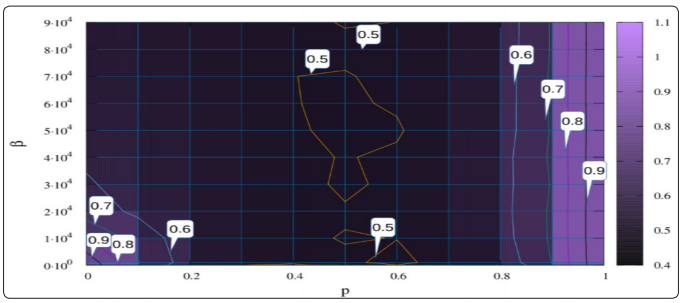


**Figure 1:** Hurst Exponent Map ($H$) depending on the feedbackpand the scale parameter $\beta$. The contours are displayed, highlighting curves for which Hurst's exponent is invariant

In the figure 2, typical fractal dimension measurements are displayed as a function of the scale parameter ($\beta$) and the feedback parameter ($p$). The fractal dimension ($D$) is a measure of roughness, while ($H$) is a quantity that classifies the diffusion regimes. The fractal dimension is related to the Hurst exponent, this relationship is described by the following equation:

$$D = \delta + 1 - H \qquad (7)$$

in which $\delta$ is the dimension in Euclidean space, in this case ($\delta$=1). The measures of ($D$) are displayed through the color map of the figure 2. The darker shades of purple are related to less rough regions than lighter regions. The lighter regions are characterized by larger measurements of the fractal dimension, therefore with greater roughness. The various shades of purple are associated with the measurements of ($D$) according to the color panel on the right side of the (Figure 2).

Note that according to the equation (7) , the fractal dimension is a result of the addition of the term (1-H) to the Euclidean dimension ($\delta$). The Euclidean dimension is a dimension without roughness, the result of the diffusive process forms a rough object whose roughness is quantified by the quantity ($D$). We have also noted that by the mathematical form of the equation (7), ($H$) and ($D$) have opposite concavities.

In the figure 2, measurements of the fractal dimension show that curves with even in the range of $1 < D < 2$. Therefore, displaying a spectrum of dimension values between an one-dimensional object and a two-dimensional object. The three-dimensional diagrams of ($H$) and ($D$) were designed as two-dimensional maps, which are presented in the figures 1 and 2 together, show a scenario that unites aspects related to diffusion regimes with roughness characteristics for our finite size random walk model. We have designed these diagrams, ($H$) and ($D$), three-dimensional in the plane ($px\beta$), noting that contour curves arise for ($H$) and ($D$), figures 1 and 2, respectively. In this analysis, we have noted that the Hurst exponent level curves, figure 1, coincide with the roughness level curves, figure 2. We have observed that larger measures of ($D$) are related to lower measures of ($H$), according to the Lorentz distribution deformations, observed when we vary the scale parameter ($\beta$).

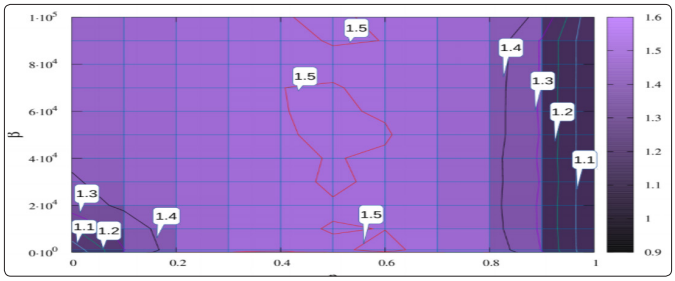


**Figure 2:** Fractal Dimension Map ($D$) in function of the feedback ($p$) and the scale parameter ($\beta$). The level curves of ($D$) are displayed, they highlight contours where roughness remains invariant to variations in ($p$) and ($\beta$).

In the figures 1 and 2, the decentralized regions in relation to the feedback parameter ($p \neq 1/2$) are overdiffused and consequently, lower roughness than the regions adjacent to ($p = 1/2$). In overdiffusion regions with ($p < 1/2$) e ($p > 1/2$) information loss occurs with increasing scale parameter. In the figure 3, information entropy measurements are presented. Information Entropy Measures Information Loss.

We have noted that as the memory access scale decreases ($\beta \rightarrow 0$), greater are the information losses. In regions of anti-persistence ($p<1/2$) and persistence ($p>1/2$), we have observed that lower information losses are associated with higher scale parameter values ($\beta$). The scale parameter is related to the random walker's ability to retrieve a past decision. Therefore, for our Lorentz memory profile finite-size walking model; the more decisions retrieved, the smaller the entropy variation ($S$); the smaller the number of decisions retrieved, the greater the entropy variation ($S$). In the persistence region ($p>1/2$), the information loss variation occurs less significantly when compared to the anti-persistence region ($p <1/2$). As we can see in the figure 3, the anti-persistence region was more sensitive, as the entropy variations, the changes of ($\beta$), than the region of persistence.

According to our numerical experiments, we have highlighte that the greatest loss of information occurs in the anti-persistence region ($\beta \rightarrow 0$) e ($p \rightarrow 0$) (figure 3), which are accompanied by the superdiffusive regime (figure 1) and smaller quantitative values of the fractal dimension when compared to the values of the adjacent regions: a ($p = 1/2$) (figure 2).

In the persistence region ($p > 1/2$), besides, we have observed at the limit of ($p \rightarrow 1$) for all values of ($\beta$), that the loss of information is accompanied by the superdiffusive regime (figure 1) and smaller quantitative values of the fractal dimension when compared to the values of the regions adjacent to ($p = 1/2$) (figure 2), but entropy variations are greater in the anti-persistence region.

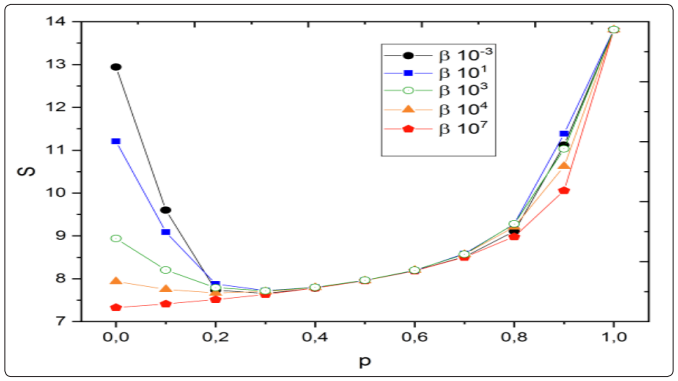


**Figure 3:** Information entropy behavior as a function of feedback parameter ($p$) and several scale parameter values ($\beta$). Each curve is obtained for a specific scale parameter. The values of the scale parameter are broken down into the range $10^{-3} \leq \beta \leq 10^{7}$.

## Discussion

So far we have talked about the physical aspects of random walking, highlighting the diffusive aspects, fractal dimension characteristics and information entropy aspects. The connection of these physical aspects with damage to the NDs perceptomotor cognitive domain is accomplished by controlling the scale parameter ($\beta$), which quantifies how effective is the random walker's ability to take back a decision from the past, for example, to bring from memory (set of variables: $\sigma_{t'}$ ) a step previously performed with probability according to the truncated Lorentz probability distribution. Therefore, the larger the scale parameter, the more memory decisions can be retrieved; the smaller the magnitude of the scale parameter, the fewer decisions can be retrieved from memory. The narrowing of the probability distribution by decreasing the scale parameter configures memory impairment, which has a consequence on the walker's praxis. The limitation of recalled memory decisions has consequences in the execution of the random walk, which presents a change in the execution of the steps quantified, when it is measured globally using Hurst's exponent. We have noted that in the persistence region several intensities of the superdiffusive regime were observed; in the anti-persistence region, similarly, several intensities of the superdiffusive regime were classified. In the region of persistence we have found curves of level of ($H$) parallel to the axis ($\beta$). Similarly, in the anti-persistence region, we have observed contours of ($H$), that intersect the axes ($p$) and ($\beta$) with downward concavity. Besides, for this two regions we have observed that the contours of the fractal dimension coincide with the curves of the Hurst exponent. However, the variations in information loss were more sensitive in the anti-persistence region than in the persistence region as the

scale parameter decreases ($\beta \rightarrow 0$), for example, the more memory damage, the more praxis-related information is lost. Therefore, the greater the memory impairment, the more affected the perceptomotor cognitive domain will be.

## References


1. Diagnostic and Statistical Manual of Mental Disorders: DSM5. 5th ed., (2013).
2. McKeith IG, Boeve BF, Dickson DW, Halliday G2, Taylor JP, et al. (2017) Diagnosis and management of dementia with Lewy bodies: Fourth consensus report of the DLB Consortium. Neurology 89: 88-100.
3. McKeith IG, Galasko D, Kosaka K, Perry EK, Dickson DW, et al. (1996) Consensus guidelines for the clinical and pathologic diagnosis of dementia with Lewy bodies (DLB): report of the Consortium on DLB International Workshop. Neurology 47: 1113-1124.
4. McKeith IG, Dickson DW, Lowe J, Emre M, O'Brien JT, et al. (2005) Dementia with Lewy bodies: diagnosis and management: third report of the DLB Consortium. Neurology 65:1863-1872.
5. Iranzo A, Fernandez-Arcos A, Tolosa E, Serradell M2, Molinuevo JL, et al. (2014) Neurodegenerative disorder risk in idiopathic REM sleep behavior disorder: study in 174 patients. PLoS One 9: e89741.
6. Toledo JB, Cairns NJ, Da X, Chen K, Carter D, et al. (2013) Clinical and multimodal biomarker correlates of ADNI neuropathological findings. Acta Neuropathol Commun 1: 65.
7. Williams SS, Williams J, Combrinck M, Christie S, Smith AD, et al. (2009) Olfactory impairment is more marked in patients with mild dementia with Lewy bodies than those with mild Alzheimer disease. J Neurol Neurosurg Psychiatry 80: 667-670.
8. Harper L, Fumagalli GG, Barkhof F, Scheltens P, O'Brien JT et al. (2016) MRI visual rating scales in the diagnosis of dementia: evaluation in 184 post-mortem confirmed cases. Brain 139: 1211-1225.
9. Bonanni L, Thomas A, Tiraboschi P, Perfetti B, Varanese S, et al. (2008) EEG comparisons in early Alzheimers disease, dementia with Lewy bodies and Parkinson's disease with dementia patients with a 2-year follow-up. Brain 131: 690-705.
10. Petrou M, Dwamena BA, Foerster BR, MacEachern MP, Bohnen NI et al. (2015) Amyloid deposition in Parkinson's disease and cognitive impairment: a systematic review. Mov Disord 30: 928-935.
11. Alafuzoff I, Parkkinen L, Al-Sarraj S, Arzberger T, Bell J, et al. (2008) Assessment of alpha-synuclein pathology: a study of the BrainNet Europe consortium. J Neuropathol Exp Neurol 67: 125-143.
12. Dickson DW, Braak H, Duda JE, Duyckaerts C, Gasser T, et al. (2009) Neuropathological assessment of Parkinson's disease: refining the diagnostic criteria. Lancet Neurol 8: 1150-1157.
13. Diniz R M B, Cressoni JC, de Silva MA A, Mariz AM. de Araújo (2017) Narrow log-periodic modulations in non-Markovian in random walks. Phys Rev 96: 062143.
14. Ingenhousz J (2010) Nouvelles expériences et observations sur divers objets de physique. T. Barrois le jeune, 1785.
15. Shütz GM, Trimper S (2004) Elefants can always remember: Exact long-range memory effects in a non-Markovian random walk. Phys. Rev 70: 045101.
16. Cressoni JC1, da Silva MA, Viswanathan GM (2007) Amnestically Induced Persistence in Random Walks. Phys. Rev. Lett 98: 070603.
17. Francis N. C. Paraan, J. P. Esguerra (2006) Exact moments in a continuous time random walk with complete memory of its history. Physical Review 74: 032101.
18. Hurst H.E, Black RP, Simaika YM, (1965) Long-Term Storage: An Experimental Study, Constable, London.
19. Walker Z, Possin KL, Boeve BF, Aarsland D (2015). Lewy body dementias. Lancet (Review). 386: 1683-1697.
20. Velayudhan L, Ffytche D, Ballard C, Aarsland D (2017) New therapeutic strategies for Lewy body dementias. Curr Neurol Neurosci Rep (Review) 17 : 68.
21. Querfurth HW, LaFerla FM (2010) Alzheimer's disease. The New England Journal of Medicine 362: 329-44.
22. Todd S, Barr S, Roberts M, Passmore AP (2013) Survival in dementia and predictors of mortality: a review. International Journal of Geriatric Psychiatry 28: 1109-1124.
23. Hsu D, Marshall GA (2017) Primary and secondary prevention trials in Alzheimer disease: looking back, moving forward. Current Alzheimer research 14: 426-440.
24. Feller W (2008) An introduction to probability theory and its applications. John Wiley & Sons.
25. K. Binder (1987) Finite size effects on phase transitions, Ferroelectrics 73: 43-67.
26. H. L. Liu, Y. G. Ma and D. Q (2019) Fang. Finite-size scaling phenomenon of nuclear liquid-gas phase transition probes, Physical Review C 99: 054614 .
27. Satya Prakash Pati, uftah Al-Mahdawi, Shujun Ye, Yohei Shiokawa, Tomohiro Nozaki, et al. (2016) Finite-size scaling effect on N´eel temperature of antiferromagnetic Cr2O3 (0001) films in exchange-coupled heterostructures Physical Review B 94: 224417.
28. A. E. Ferdinand, M. E. Fisher (1969) Bounded and Inhomogeneous Ising Models. I. Specific-Heat Anomaly of a Finite LatticePhys. Rev 185: 832.
29. D.P. Landau (1976) Finite-size behavior of the Ising square lattice. Phys. Rev 13: 2997.
30. K Binder (1981) Critical Properties from Monte Carlo Coarse Graining and Renormalization. Phys. Rev. Lett 47: 693-696.
31. D.P. Landau, K. Binder (1985) Phase diagrams and critical behavior of Ising square lattices with nearest-, next-nearest-, and third-nearest-neighbor couplingsPhys. Rev. B 31: 5946-5953.
32. V Privman (1990) Finite-Size Scaling and Numerical Simulations of Statistical Systems. World Scientific, Singapore.
33. Shannon C E (1948) A Mathematical Theory of Communication. Reprinted with corrections from The Bell System Technical Journal 27: 379-423.